CFD ANALYSIS OF THERMAL BEHAVIOR WITHIN A SCRAPED SURFACE HEAT EXCHANGER (SSHE)

Rajesh S C, Dr. B. Sadashive Gowda, Dr. G.S.V.L. Narasimham

VVPIET Solapur, rajesh.sc044@gmail.com

Abstract: This paper deals with Computational Fluid Dynamic (CFD) analysis of 3D model of an SSHE is developed in order to study the fluid flow and heat transfer with a steady state laminar, non-isothermal flow of pure glycerine, which can be treated as a newtonian fluid. The variation of the local heat transfer coefficient based on the inner wall temperature and bulk fluid temperature as a function of the main process parameters, namely, rotational Reynolds number (Re_{rot}), axial Reynolds number (Re_{axi}) and dimensionless clearance, is obtained. The results have shown that viscous dissipation has a significant effect on the cooling of glycerine. The local heat transfer coefficient increases slightly when the tip clearance increases. Larger increases of the same occurred with higher rotational Reynolds number and axial Reynolds number. A correlation of the average Nusselt number is obtained in terms of the rotational and axial Reynolds numbers. This is expected to be useful in the design of SSHEs handling highly viscous fluids.

Keywords: Scraped surface heat exchanger, Newtonian fluid, Inner wall temperature, Bulk fluid temperature,

Local heat transfer coefficient, Nusselt number, dimensionless tip clearance

1. INTRODUCTION

SCRAPED SURFACE HEAT EXCHANGER (SSHE) is a device which consists of an annular gap with a cylindrical rotor and stator as shown in Fig 1. Scraping means removal of fluid from the boundary. This breaks the thermal and hydrodynamic boundary layers at the surface and there by enhances the heat transfer. Specifically an SSHEs is used for the thermal treatment of high-viscous fluids. SSHE is widely used in food industry for sterilizing or cooling highly viscous fluids such as mayonnaise, cream cheese, peanut butter and ice cream. As the treated fluids in SSHE are highly viscous, fouling problems may occur and reduce significantly the thermal efficiency of SSHE. The presence of rotating blades in the annulus makes it possible to avoid the possible fouling problem on the heat exchanger surface, and improve the heat transfer treatment received by the product. A short discussion of the previous studies of authors who attempted to focus on the heat transfer and basic flow patterns in SSHE is presented here. Trommelan et al. [1] was the first person to describe the fluid flow and heat transfer mechanisms for the design and operating conditions of the SSHE. The presence of blades in the annulus makes the fluid flow more complex compared to the Coutte-Taylor flow configurations with a blade clearance of 1µm. Penny and Bell [2] suggested that the clearance between the edge of the scraper blade and the stator wall is not constant, but it is dependent on the operating conditions of the SSHE. De Gode et al. [3] studied the freezing of water-ethanol slurries using an ice generator with a blade clearance of 3 mm and 1 mm, to examine the heat transfer coefficient on the exchanger surface. Toh and Murikami [4] studied the shape of two scraper blades, one curved and another, perpendicular to the wall. Bott and Ramero [5] numerically studied an SSHE to compare the overall heat transfer coefficient with different numbers of scraper blades like 2, 4 and 6. The study shows that increasing the number of scraper blades increases the power consumption and that there are no advantages in increasing the number of scraper blades beyond four. Yataghene et al. [6] conducted a numerical study of the fluid flow and heat transfer within a SSHE, using 130 µm clearance of the blade gap with pure glycerin fluid and examined the mixing time for the exit temperature of the SSHE. Harrod [7] studied the SSHE using a newtonian fluid (water). One of the key purposes of the paper was to model the heat transfer for both laminar and vertical rotational flow, to find the transition between laminar and vertical flow. D'Addio [8] analyzed the thermal behavior of a new kind of SSHE with an alternate scraper blades arrangement, namely, A-SSHE, during the heating and cooling of hazelnut paste, which is a high viscous fluid. He determined the heat transfer coefficient by varying rotational Reynolds number (5 < Re < 250), axial Reynolds number (0.06, 4) and Prandtl number (6800, 60000). Stranzinger et al. [9] studied the flow pattern in SSHE, using experimental flow visualization (PIV technique) in a simplified geometry (blades fixed on the stator) and numerical simulation based on finite volume method (FVM). Hartel [10] gave a review of the SSHE in which particular attention was given to the crystallization process of ice cream. He concludes that the mechanical energy dissipated can reach 50% of the calorific energy evacuated by the cooling fluid. More recently viscous heating within SSHE was investigated by Fayolle et al. [11]

both experimentally and numerically. They found that for Newtonian fluid with high viscosity, the effect of viscous heating was very important.

All though work is reported in the literature on the topic of heat transfer in a SSHE, the conjugate heat transfer due to finite wall thickness of the stator has not received much attention. Moreover issues like inner wall temperature, bulk fluid temperature and local heat transfer coefficient for the thermally fully developed flow and the effect of the clearance between the tip of the blade and the stator wall have not been clearly addressed.

The objective of the present work is to create a 3D model of an SSHE and study the fluid flow and heat transfer in steady state laminar non-isothermal flow of pure glycerine (newtonian fluid) with temperature dependent viscosity. The clearance between tip of the blade and the stator is taken as $\delta_{gap} = 2$mm, and 65µm. The relevant dimensionless numbers for the present study are the Rotational Reynolds numbers (Re_{rot}), axial Reynolds number (Re_{axi}) and the dimensionless clearance. The four rotational Reynolds numbers (Re_{rot}) investigated are 26.39, 79.17, 158.39, 237.61 and the axial Reynolds numbers (Re_{axi}) are 0.6, 1.21, 1.82, and 2.43. Parametric study is done by keeping the rotational Reynolds number constant and varying the axial Reynolds number (Re_{axi}), and repeating the same procedure as above for different (Re_{rot}). Thus for each clearance, 16 simulations are to be performed and for three different clearances, 48 simulations are to be carried out. The local heat transfer coefficient for the heat exchanger surface is based on the inner wall temperature and bulk fluid temperature for each cross section of the SSHE. The parameters for which thermally developed flow occurs are examined.
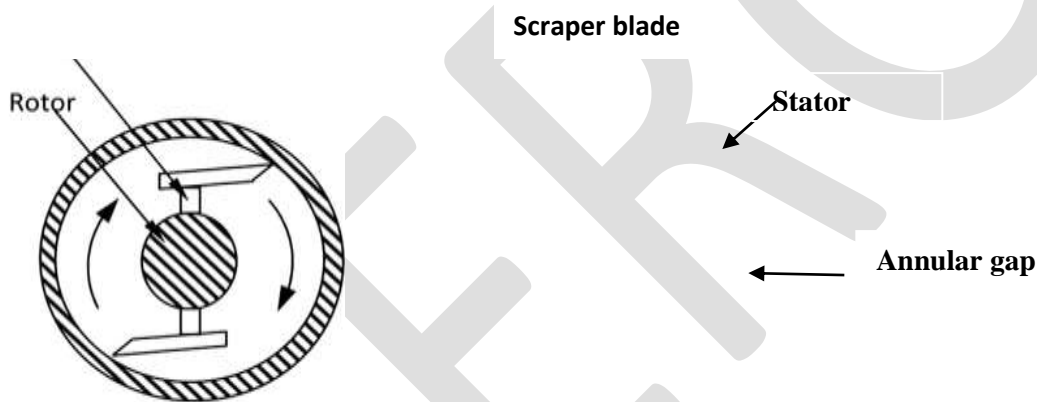

Fig 1: Transversal cross-section of SSHE [6]

2.   MATHEMATICAL FORMULATION

2.1 The physical model and coordinate system

A 3D model of SSHE is created in Gambit (Ver. 2.4.6). In view of the geometry, the Cartesian co-ordinate system is chosen to describe the geometry, where X, Y and Z axis are taken in the horizontal, vertical and axial directions of the SSHE respectively. The model is shown in Fig. 2.
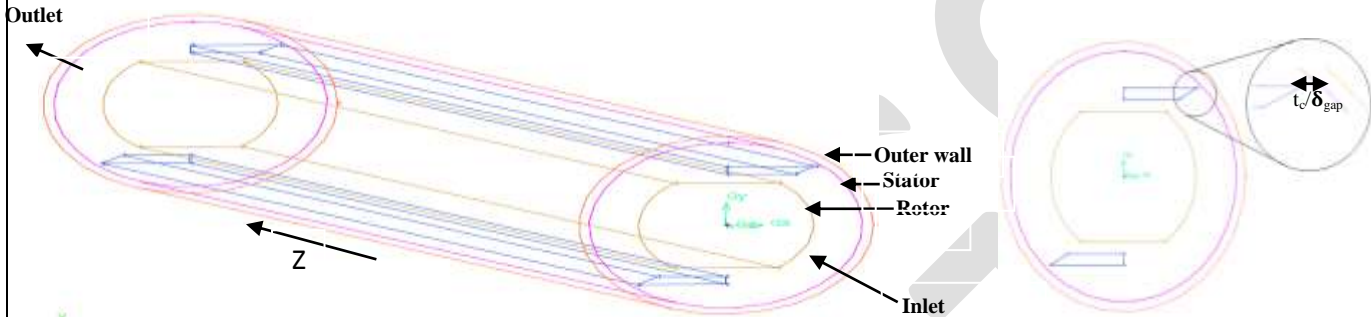

Fig 2: 3D model of SSHE with 2mm clearance

The SSHE consists of a rotor with two fixed scraper blades. The stator surface represents the wall heat exchanger, where a constant wall temperature is applied to the outer wall. In this study the three different clearances between the tip of the blade and stator wall are 2 mm and 65 µm. Other dimensions of the SSHE device are: stator diameter (Ds) =0.065m, rotor diameter (Dr) =0.040m, stator length (Ls) =0.6m, number of blades (n) =2, area of cross section =2.945e-3 m², and number of blades (n) = 2.

3.   GRID INDEPENDENCE STUDY

A commercially available meshing tool is used to generate good quality hexagonal grids. A structured mesh overlaying the hexahedral elements is generated with the Gambit (Ver. 2.4.6) software meshing tool. The mesh density is increased near the wall and especially in the clearance region to ensure accuracy there, as greater temperature changes in the fluid are expected to occur in these regions. The mesh is highly concentrated at the tip of the blades and ensured there were at least 4 mesh points across the tip of the clearance. This was done by performing a number of simulations with different mesh sizes, starting from a coarse mesh and refining it until physical results were no more dependent on the mesh size. The hexahedral cells were retained to have good discretization accuracy. Four mesh refinements of 663600, 831600, 979200 and 1248000 cells were tested and compared with a physical parameter of bulk temperature of the fluid for each cross section of SSHE as shown in Fig 4. For good accuracy of the results, the case with 979200 cells can be employed as this gives no significant difference compared to that with 1248000 cells. A fine mesh of 979200 cells is chosen for further analysis as shown in Fig. 3.
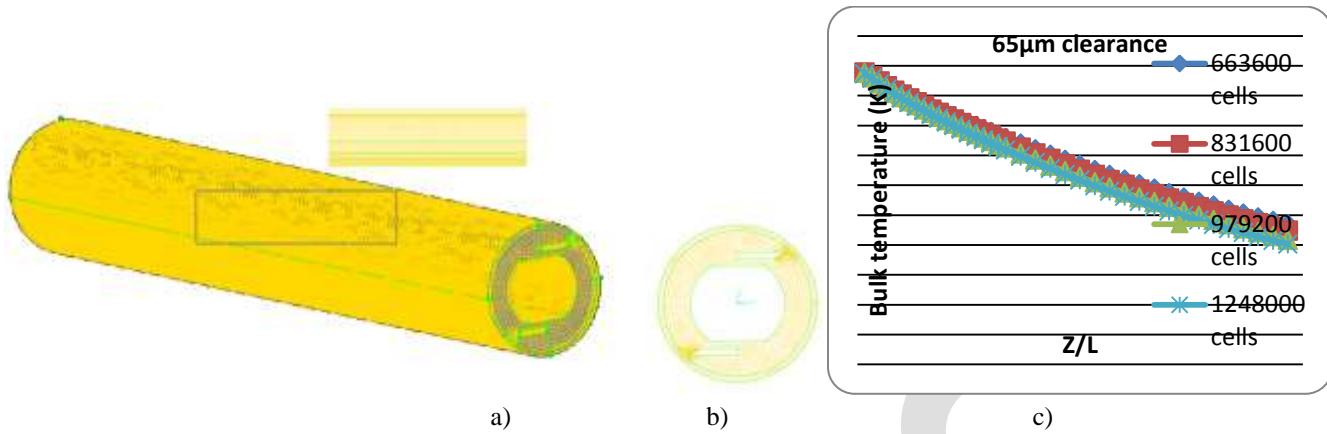
Figure 3: a) Computational of physical domain of a SSHE and used grid, all physical domains was meshed with hexahedral cells of (1279200) b) SSHE Transverse cross section of the mesh topology of physical c) Variation of bulk fluid temperature for different mesh cells for 65µm clearance.

4. GOVERNING EQUATIONS

In this section the governing equations are stated for the heat transfer and fluid flow including viscous dissipation in the SSHE. Steady state, non-isothermal, incompressible flows have been considered. The flow is assumed to be laminar in the entire computing fluid domain with rotation Reynolds number lower than 250 and axial Reynolds number lower than 4. The conservation equations for continuity, momentum and energy for incompressible flows have been solved in dimensional form. It is pertinent to use the rotating reference frame formulation to solve the continuity, momentum and energy equations. The principal reason for employing moving reference frame is to render a problem which is unsteady in the stationary (inertial) frame steady with respect to the moving frame.

In the rotating reference frame, the continuity equation in steady state for the relative velocity is written as:

$$\nabla\left(\vec{v}_r\right)=0 \tag{1}$$

The momentum equation is written as:

$$\nabla\left(\vec{v}_r\,\vec{v}_r\right)+\left(2\,\vec{\omega}\times\vec{v}_r\right)+\left(\vec{\omega}\times\vec{\omega}\times\vec{r}\right)=-\nabla p+\nabla\vec{\tau}_r \tag{2}$$

Momentum equation contains two additional acceleration terms: the coriolis acceleration $\left(2\,\vec{\omega}\times\vec{v}_r\right)$ and the centripetal acceleration $\left(\vec{\omega}\times\vec{\omega}\times\vec{r}\right)$

Energy equation for the fluid in steady state for rotating frame is expressed as:

$$\underbrace{\nabla\left(\vec{v}_r.H_r\right)}_{\text{Forced heat convection}}=\underbrace{\nabla\left(k\nabla T\right)}_{\text{Heat conduction}}+\underbrace{\nabla\left(\vec{\tau}_r\,\vec{v}_r\right)}_{\text{Viscous heating}} \tag{3}$$

In the present work we will neglect the effects of gravity; however, it is straightforward to include it in the axial pressure gradient if the SSHE is mounted with the axis vertical. The stator wall (heat exchange surface) was taken into account with 5 mm thickness. The energy equation has been solved in the fluid and the conduction equation in steady state applicable to solid regions is:

Energy equation for solid:

$$\nabla.\left(\rho_{steel}C_{psteel}(-\omega \times r)T\right) = \nabla\left(k_{steel}\nabla T\right) \qquad (4)$$

The system of non-dimensionalisation is:

$$\text{Re}_{axi} = \frac{v_{in}d_{equ}\rho}{\eta} \quad \text{Re}_{rot} = \frac{\omega.d_{equ}\rho}{\eta} \quad \text{Pr} = \frac{\eta c_p}{k}$$

5. BOUNDARY CONDITIONS

We have examined in this work the fluid cooling process occurring in an SSHE. For the fluid flow, the momentum equation (Eq. 3) boundary conditions are specified as follows: On the stator: $v = \omega \times r$. At the rotor and scraper blade: $v = 0$. Flow at inlet : v_{in} m/s. Outflow: zero velocity gradient $\partial v/\partial n=0$. The fluid (glycerine) is introduced at the SSHE inlet with the temperature of T_{inlet}=288K, and was cooled with the constant outer wall temperature T_w=278K. The temperature difference between the wall heat exchanger and fluid inlet was ΔT=10K. Adiabatic conditions were assumed for the rotor and scraper blade. Zero temperature gradient is assumed at the outlet.

ANSYS Fluent code uses the finite volume method for discretization. The governing steady-state equations for mass and momentum conservation are solved with a segregated approach. In this approach, the equations are sequentially solved with implicit linearization. Volume-faces advective fluxes were approximated using a second- order upwind interpolation scheme. Because of the effect of the viscosity variation due to heat transfer, a coupling between velocity and temperature fields must be considered. The pressure-velocity coupling is implemented using iterative correction procedure (SIMPLEC algorithm). For the energy equation too, a second-order upwind interpolation scheme is used.

6. CODE VALIDATION

The problem is solved using Fluent CFD code. In order to check for the accuracy and correctness of the code, the results of Yataghene [9] are reproduced. The problem deals with the CFD analysis for various rotational velocities with a constant volumetric flow rate. The dimensionless exit temperature is calculated using Eq. (7) for pure glycerin by varying rotational velocities in the range 3-10 rev/s. Fig. 4 shows the comparison of the results of Yataghene[9] and the present Fluent results. From this we can comment that the variations are almost identical except that the present results show slightly higher values. This level of agreement is considered satisfactory. It may be noted that when increasing the rotational velocities, the temperature is increases due to viscous dissipation of the fluid.

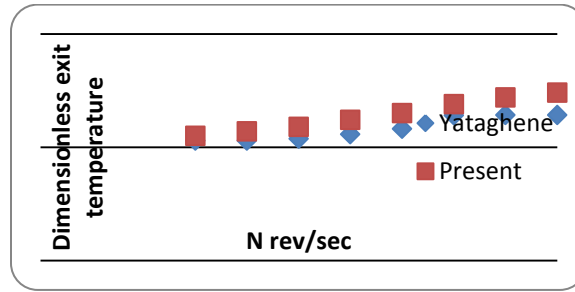$$\theta = \frac{T_{out} - T_{wall}}{T_{in} - T_{wall}} \qquad (5)$$

Fig 4: Comparison of temperature contours

7. RESULTS and DISCUSSION

In order to obtain the performance characteristics of 3D model of SSHE for the fluid flow and heat transfer, a parametric study is carried out by varying the clearance between the tip of the scraper blade and the stator wall, the angular velocity of the rotor and the axial velocity of the fluid entering the SSHE. The dimensionless parameters corresponding to the above dimensional parameters are the dimensionless tip clearance, the rotational Reynolds number (Re_{rot}) and the axial Reynolds number (Re_{axi}). Contour plots are constructed to depict the flow and temperature distributions. Graphs are plotted to show the variation of inner wall temperature, bulk temperature and the local heat transfer coefficient. The local heat transfer coefficient is calculated with Eq. (8) with respect to the axial distance. Correlations are obtained for the average Nusselt number based on the average heat transfer coefficient in terms of the process parameters.

$$h = \frac{q_w}{T_{in,w} - T_{bulk}} \qquad (6)$$

7.1 Flow and temperature distributions

Figs. 5 (a, b) show the temperature contours for the axial position corresponds to the near-exit section (Z=0.55 m) of the SSHE, for various dimensional clearances. The color code gives information about the temperature limits, the blue color corresponding to 278 K and the red corresponding to 288 K. In Fig (5a), corresponding to 2 mm clearance, the hot fluid is more located in the core and the extent of cooled fluid is very less. Hence higher blade clearance does not produce effective cooling of the fluid. When we observe Figs. 5 (b) for 65 µm clearance, better cooling process of the fluid takes place with a proper distribution of the cooling temperature is achieved with decreasing the tip of the clearance and there is good heat removal at the boundary surface.
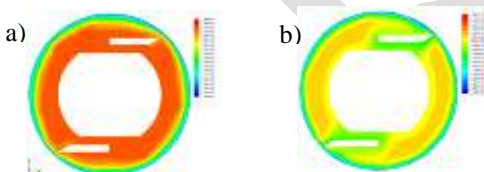
a)

b)

Fig. 5 Temperature contours of SSHE cross section in case of Z=0.55 m a) 2 mm clearance b) 65 µm clearance Re_{rot}=237.13 and Re_{axi}=0.0188

7.2 Axial variations of temperature difference and local heat transfer coefficient

The inner wall temperature and bulk fluid temperature distributions along the SSHE axial distance are shown in Figs. 6 (a, b) at different values of axial Reynolds number, rotational Reynolds number and also for different dimensionless tip clearances. For 2 mm clearance with a rotational Reynolds number (Re_{rot}) of 158.39, the inner wall temperature is very high at the inlet section and the temperature of the inner wall gradually decreases along the axis of the SSHE. When comparing the two curves of the inner wall temperature and the bulk fluid temperature at different axial Reynolds number (Re_{axi}), it can be seen that these two lines are almost parallel to each other and we can say that the temperature difference is uniformly distributed to the fluid. At the tip clearances of 65 μm, the scraper blades continuously remove the boundary layer surface and better cooling occurs with the inner wall and bulk temperatures decreasing with axial distance along the SSHE. When increasing the rotational Reynolds number, the inner wall temperature and bulk fluid temperature increase due to viscous dissipation, which in turn decreases the viscosity of the fluid.
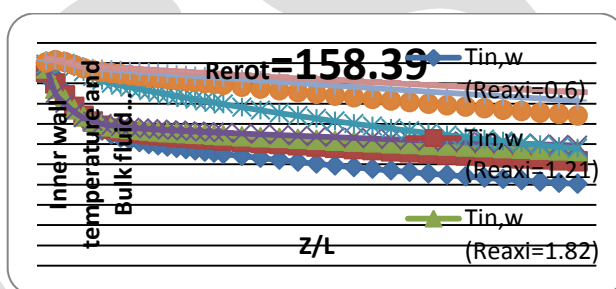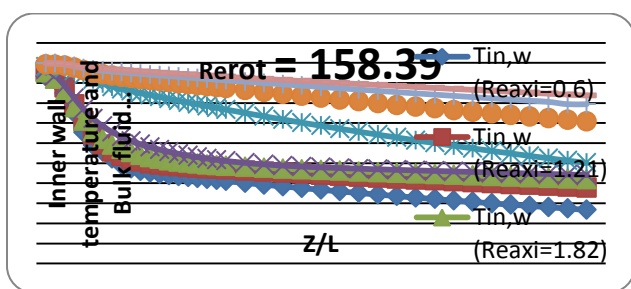

Fig. 6(a) Inner wall temperature and bulk fluid temperature

Fig. 6(b) Inner wall temperature and bulk fluid temperature for 65 μm clearance with different axial Reynolds number

The local heat transfer coefficient based on inner wall temperature and bulk fluid temperature calculated using Eq. (8) along the axial distance of SSHE is shown in Figs. 7 (a, b) for different Reynolds numbers and also for different tip clearances. The general variation of local heat transfer coefficient reveals that it is of high value near the inlet section of the exchanger because of the thickness of the boundary layer is very small. It decreases continuously due to the increasing thermal boundary layer thickness. When the dimensionless tip clearance decreases (i.e., 65 μm as against 2 mm clearance), better local heat transfer coefficient is achieved and improvement in the performance of the SSHE is obtained. It can be observed in Fig. 8(a) (2 mm clearance) that the local heat transfer coefficient is less compared to the other clearance. This is because the scraper blades only brush against but not scrape the exchanger surface. When tip clearance decreases, the scraper blades remove the boundary layer and result in higher values of local heat transfer coefficient. A thermally fully developed flow of the fluid is also achieved.
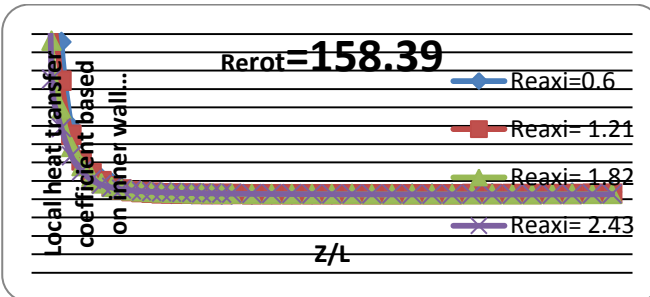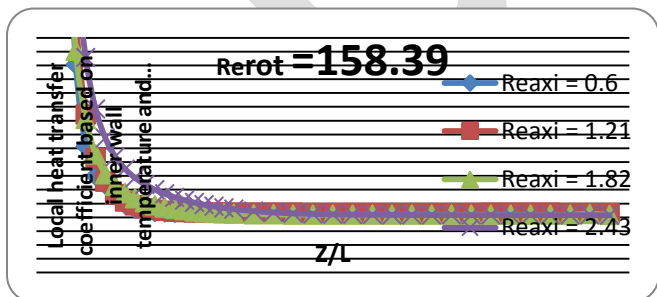

Fig. 7(a) Local heat transfer coefficient based on inner wall temperature and bulk fluid temperature for 2 mm clearance with different axial Reynolds number

Fig 7(b) Local heat transfer coefficient based on inner wall temperature and bulk fluid temperature for 65 μm clearance with different axial Reynolds number

7.3 Correlations for average Nusselt number

The following correlation has been established for average Nusselt number by using the Eq. (9) under several operating conditions of SSHE.

$$Nu_{avg} = \frac{\bar{h}\,d_{equ}}{k} \qquad (7)$$

In obtaining the heat transfer correlation, the rotational and axial Reynolds numbers are taken as parameters. The Prandtl number variation does not occur because results are obtained for only a single fluid, namely, glycerine.

The correlation obtained using multiple regression analysis is:

$$Nu = a\,\mathrm{Re}_{rot}^{b}\,\mathrm{Re}_{axi}^{c} \qquad (8)$$

where a, b and c are the constants of the correlation. In order to determine the constants a, b and c of the model several numerical simulations were carried out. Figs. 8 (a, b) show the parity plots between computed and correlated Nusselt number in which 16 data points pertaining to one dimensionless clearance are shown for each plot. Although not presented, similar plot is also obtained for the remaining clearance. The correlation constants are given in Table 1:
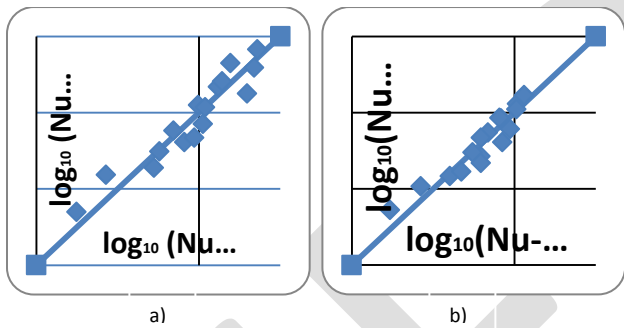

a) b)

Table 1: Correlation constants

Correlation constants	2 mm Clearance	65 μm Clearance
a	51.62	58.40
b	0.06	0.10
c	0.15	0.19
R^2	0.94	0.95

Fig. 8 Parity plots between computed and correlated values of

Nusselt number for a) 2 mm clearance b) 65 μm clearance

According to obtained results it appears that the increase of the rotating speed improves the efficiency of the SSHE for all considered dimensionless clearances.

8. CONCLUSIONS

A 3D CFD model is employed to examine the thermal performance of an industrial scraped surface heat exchanger device. A parametric study is done and the following conclusions are reached:

1) The difference between inner wall temperature and bulk fluid temperature increases due to viscous dissipation of the fluid.

2) The local heat transfer coefficient based on inner wall temperature and bulk fluid temperature increases along the length of the SSHE in the axial direction with decreasing tip clearance.

3) In case of 2 mm clearance, the local heat transfer coefficient is very less compared to other clearance because the scraper blade only brushes but does not to scrape the surface. For 65μm clearance, the scraper blades scrape the boundary layer at the surface and this increases the local heat transfer coefficient.

4) The local heat transfer coefficient increases with increasing rotational Reynolds number; this improves the performance of the SSHE.

5) A heat transfer correlation is obtained for the average Nusselt number in terms of the rotational and axial Reynolds numbers, which are the process parameters.

REFERENCES:

[1] **Trommelen A. M, Beek W. J**, "Flow Phenomena in a Scraped Surface Heat Exchanger ("votator" type)", *Chem. Engg Sci*, Vol. 26, No. 11, pp 1933-1942

[2] **Penney W. R, and Bell K. J**, *Ind. Engng Chem.* 1967 59 (apr) 40.

[3] **De Goede R, De Jong E. J**, "Heat Transfer Properties of Scraped Surface Heat Exchanger in the turbulent Flow Regime", *Chem. Eng. Sci.* Vol. 48, No. 1993, pp 1393–1404

[4] **Toh and Murikami. Y, (1982)**, "Power Consumption of a Fluid Loaded Floating Scraper Blade", *J Chem Engg JPN.* Vol. 15, No. 6, pp 493

[5] **Bott T. R, Romero. JJB, (1966)**, "The Characteristic Dimension in Scraped Surface Heat Exchanger. *J Chem Engg*, 44, 226.

[6] **Mourad Yataghene. Jack Legrand**, "A 3D-CFD model thermal analysis within a scraped surface heat exchanger," *Chem Engg*. Vol 71, No.2013, pp 380-399.

[7] **Härröd. M, (1987),** "Residence time distribution, heat transfer and power requirements," Journal of Food Process Engg 9: 1-62

[8] **D'Addio. L, Dejong E. j, 1993**, "Heat Transfer Properties of a Scraped Surface Heat Exchanger in the Turbulent Flow Regime," *Chem, Engg, Sci*," Vol No, 48, pp 1393-1404.

[9] **Stranzinger M, Feigl k, Windhab E**, "Newtonian Flow Behavior in Narrow Annular gap Reactors," *Chem Eng Sci* 2001, Vol. 56, No. 11, pp. 3347-3363

[10] **Hartel R. W**, "Ice Crystallization during Manufacture of Ice Cream", *Trends Food Sci Technol* 1996, Vol. 7, No. 10, pp 315-321

[11] **Fayolle F, Legarand J**, "Experimental and numerical analysis of heat transfer including viscous dissipation in a scraped surface heat exchanger" *Chem Eng process*, Vol. 2009, No. 48, pp 1445-1456